Electronic Supplementary Material (ESI) for Green Chemistry.
This journal is © The Royal Society of Chemistry 2019

SUPPORTING INFORMATION

Hydrothermally stable $ZnAl_2O_4$ nanocrystals with controlled surface structures for design of longevity and highly active/selective PdZn catalyst

Xian-Hua Zhang,[*a] Chang Liu,[a] Congming Ke,[b] Liang Liu,[a] Xinning Hao,[a] Yaping Wu,[*b] Shaolong Wan,[a] Shuai Wanga and Yong Wang[*c]

a. Department of Chemistry, College of Chemistry and Chemical Engineering, State Key Laboratory for Physical Chemistry of Solid Surfaces, National Engineering Laboratory for Green Chemical Production of Alcohols-Ethers-Esters, Xiamen University, Xiamen 361005, People's Republic of China

b. Department of Physics, OSED, Fujian Provincial Key Laboratory of Semiconductor Materials and Applications, Jiujiang Research Institute, Xiamen University, Xiamen 361005, People's Republic of China

c. Voiland School of Chemical Engineering and Bioengineering, Washington State University, Pullman, WA 99164, USA

SUPPORTING INFORMATION

Table of Contents

Experimental Procedures

1. Materials. Aluminum (III) nitrate nonahydrate (≥99.0 %), Zinc (II) nitrate hexahydrate (≥99.0 %), Palladium (II) nitrate dihydrate (Pd~40%), Sodium hydroxide (≥96.0 %), nitirc acid (65.0%~68.0%), isopropanol (≥99.7 %) and glycerol (≥99.0 %) were purchased from Sinopharm Chemical Reagent Co. Ltd. China. All chemicals were used as received without further purification.

2. Synthesis of Zn-rich or Al-rich $ZnAl_2O_4$ nanocrystals. 15.0 g aluminum nitrate nonahydrate and 6.5 g zinc nitrate hexahydrate for Zn-rich sample (Zn/Al ratio of 1.1/2) or 5.5 g zinc nitrate hexahydrate for Al-rich sample (Zn/Al ratio of 0.9/2) were dissolved in 100 mL isopropanol respectively. The mixture was stirred for about 1h to form a clear solution, then the solution was transferred into a steel autoclave with a 150-mL teflon inner. The autoclave was placed in a programmed oven and heated at 200 °C for 24h. The precursor mixture was centrifuged to remove solvent (reusable), and dryed at 150 °C. The obtained powder was heated at 600 °C for 5h, then nano-sized $ZnAl_2O_4$ powder was dispersed into 20 mL diluted nitric acid (~5 wt%) or NaOH solution (1 M), stirring overnight. Finally, the mixture was centrifuged and washed by deionized (DI) water until no change in pH. After centrifugation and dried procedures, the obtained powder was collected for characterizations.

3. Synthesis of nanostructured Al_2O_3. Nanostructured Al_2O_3 was synthesized by the same procedures as the synthesis of $ZnAl_2O_4$ nanocrystals, except that aluminum nitrate nonahydrate was used as the Al_2O_3 precursor and no washing procedures (HNO_3 or NaOH) was used.

4. Synthesis of PdZn/$ZnAl_2O_4$ nanocatalyst. 0.5 g $Pd(NO_3)_2{\cdot}2H_2O$ was dissolved into 62.5 mL HNO_3 (65.0~68.0 wt%), and diluted to a 500 mL solution with deionized water, then a clear stock solution was obtained by sonication. The spinel supported Pd catalysts with varied Pd loadings were prepared by the incipient wetness impregnation method. Briefly, 1.25 mL stock solution was added onto 1 g $ZnAl_2O_4$ supports by droplet, then deionized water was added to a 30 mL mixture stirring overnight. Slurry was formed by stirring at 80 °C followed by drying at 100 °C. The obtained powder was sintered at 400 °C for 3 h to obtain PdZn catalyst (0.1wt%PdZn/$ZnAl_2O_4$).

5. Hydrothermal testing. About 1.0 g of sample was loaded along with 15 mL of deionized water into a 20-mL autoclave with Teflon inner. The autoclave was transferred into a preheated oven at 200 °C and left for the desired treatment duration (1 ~ 14 days) after which the autoclave was removed and allowed to cool down to room temperature. The resulting hydrothermal treated samples were collected by filtration with deionized water, recovered, and dried in a heating oven (100 °C) before characterization.

6. Catalytic testing. Catalytic tests were carried out in a 100 mL stainless steel autoclave with stirring at a speed of 700 rpm. 5 g of glycerol was added into 45 g of deionized water for a 10 wt % glycerol solution. Pd-based catalysts (i.e., PdZn/$ZnAl_2O_4$) were added to the glycerol aqueous solution. The autoclave was flushed with H_2 (>99.99%) more than three times after fully purging out the air and thenpressurized to 5.0 Mpa, followed by heaing to the reaction temperature (220 °C) monitored by a thermocouple inserted into the autoclave. The concentrations of glycerol and hydrogenolysis products were analyzed by high-performance liquid chromatography (HPLC; Angilent 1260) equipped with double detectors (RID and UV-Vis) and Bio-Rad Aminex HPX-87H ion exclusion column (0.005 mol/L H_2SO_4 mobile phase, 0.6 mL/min flow rate, and 70 °C oven temperature). For cyclic stability tests, the used catalysts were washed three times with deionized water, three times with ethyl alcohol, and then dried in a drying oven at 80 °C for 4h before the next cycle test.

7. Characterizations. XRD patterns were collected on a X-ray powder diffractometer with D/Tex Ultra 1-D Silicon Diaray Detector (Ultima IV, Rigaku Co., Japan) in the 2θ range of 10-90° using Cu Kα1 radiation (λ = 1.5406 Å) operated at 40 kV and 30 mA. Particle size analysis was conducted by the attached software (PDXL2). X-ray photoelectron spectroscopy (XPS) analysis was carried out on a VG Multilab 2000 spectrometer (Thermo Electron Corporation, USA) with Al Kα radiation as the exciting source (300 w). SEM experiments were performed using a HITACHI S-4800 Field Emission Scanning Electron Microscope with accelereted voltage max. 30 kV (HITACHI Ltd., Japan). TEM , HRTEM and EDX analyses were performed using a Philips TECNAI F30 attached with an EDX system (Philips-FEI Co. Netherlands). XRF analysis was carried out on wavelength dispersive X-ray fluorescence spectrometer (S8 Tiger, Bruker Co., German), and pellet diameter was 28 mm. The nitrogen adsorption and desorption isotherms at the temperature of liquid nitrogen were measured using a Micromeritics ASAP 2020Plus system (Micromeritics Instrument Ltd., USA). The samples were outgassed for 10 h at 350 °C before the measurements. The pore-size distribution for mesopores was calculated by Original Density Functional Theory. The samples were pretreated at 383 K for 12 h under vacuum. The surface areas were determined from adsorption values for five relative pressures (P/P_0) ranging from 0.05 to 0.2 using the BET method. CO-chemisorption was performed by the chemical module of ASAP 2020Plus at 308 K and with CO flow of 70 mL/min. The thermal diffusivity was investigated in a laser flash apparatus (LFA447/2-4Insb NanoFlash, Netzsch Geratebau GmbH, German) from 25 °C-250 °C under helium atmosphere, powder sample was pelleted under 1T pressure and the pellets (Φ 12.7 mm, thickness 2 mm) were covered by a thin graphite layer to ensure a sufficient absorption of the laser light.

8. Computational Methods. Energy stability of all surfaces and adsorption configurations were analyzed using the plane-wave DFT, as implemented in the Vienna ab initio simulation package (VASP)**[1]** code with the projector augmented wave (PAW) basis sets.

The cell of $ZnAl_2O_4$ was constructed based on atomic coordinates from PDF card (01-071-0968). A 15 Å vacuum layer along the *z* direction was constructed to minimize artificial interactions between neighboring slabs. The valence electron configurations of Zn, Al, O and H atoms are $3d^{10}4s^2$, $3s^23p$, $2s^22p^4$ and $1s$, respectively. Generalized gradient approximation (GGA)**[2]** with Perdew-Burke–Ernzerhof (PBE)**[3]** parameterization was employed to descript the exchange-correlation. Electron wave functions were expanded in plane waves with an energy cutoff of 520 eV. The Brillouin zone was sampled with a 9 × 9 × 1 Monkhorst-Pack grid of *k* points. All atomic degrees of freedom, including lattice parameters, were fully relaxed with electronic iteration convergences of 0.01eV $Å^{-1}$ and 1×10^{-4} eV for force and energy, respectively. The surface dangling bonds on the lowermost atomic layer of each polar surface were saturated by hydrogen-like atoms to eliminate an unphysical transfer of charge between the top and bottom sides of the slab. Explicitly, the artificial atoms with a fractional nuclear charge of 3/2, 5/4 and 1/2 were added for Zn-, Al- and O- terminated surfaces, respectively.

Table S1. The results of theoretical calculations

facets	Zn-ended or Al-ended	Zn-OH or Al-OH	OH	ΔE
(100)	Zn-ended	Zn-OH	OH	ΔE
	-374.90 eV	-386.45 eV	-7.12 eV	-4.43 eV
	Al-ended	**Al -OH**	**OH**	**ΔE**
	-370.15 eV	-386.23 eV	-7.12 eV	-8.96 eV
(110)	**Zn-ended**	**Zn-OH**	**OH**	**ΔE**
	-195.975eV	-206.80eV	-7.12eV	-3.725eV
	Al-ended	**Al-OH**	**OH**	**ΔE**
	-195.975eV	-207.338eV	-7.12eV	-4.243eV

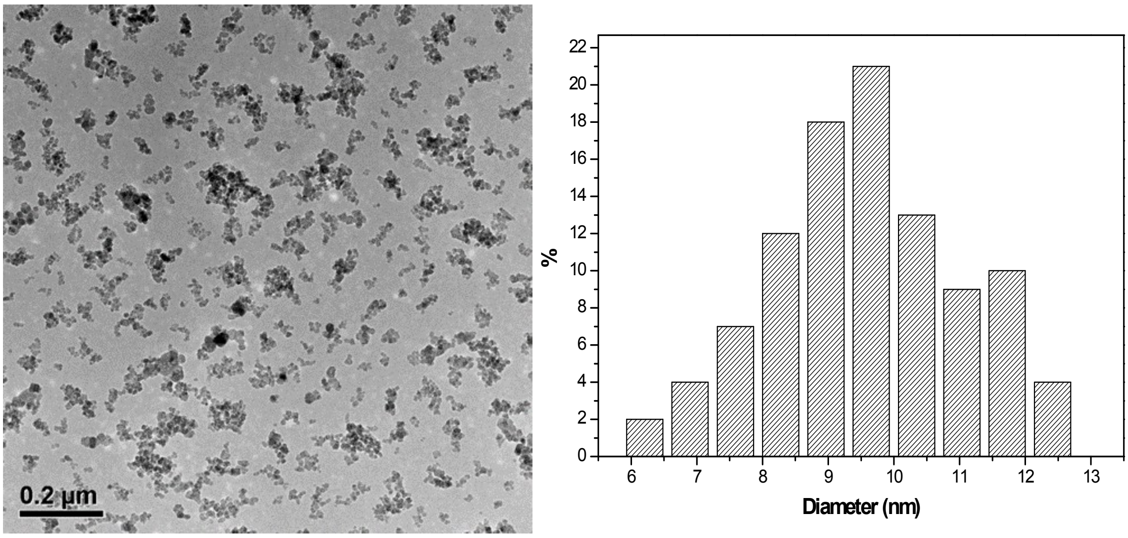

Fig. S1 TEM image of $ZnAl_2O_4$ nanocrystals after hydrothermal test, and diameter distribution of nanocrystals by TEM analysis.

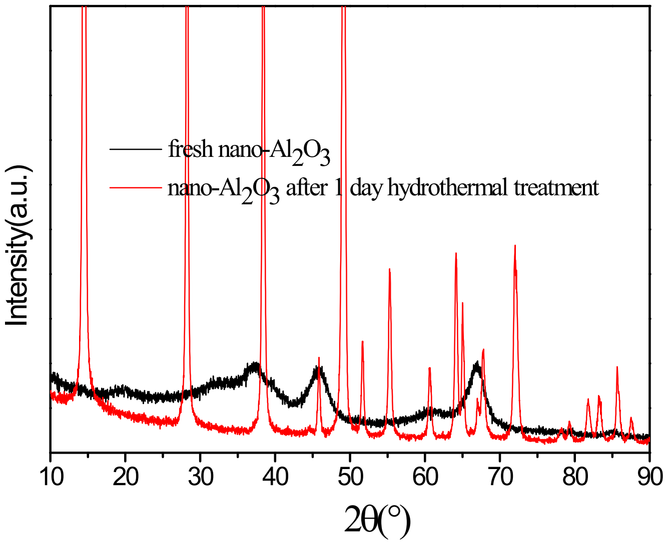

Gamma Al_2O_3	AlO(OH)
Average size (Å)	Average size (Å)
69.9	576.5

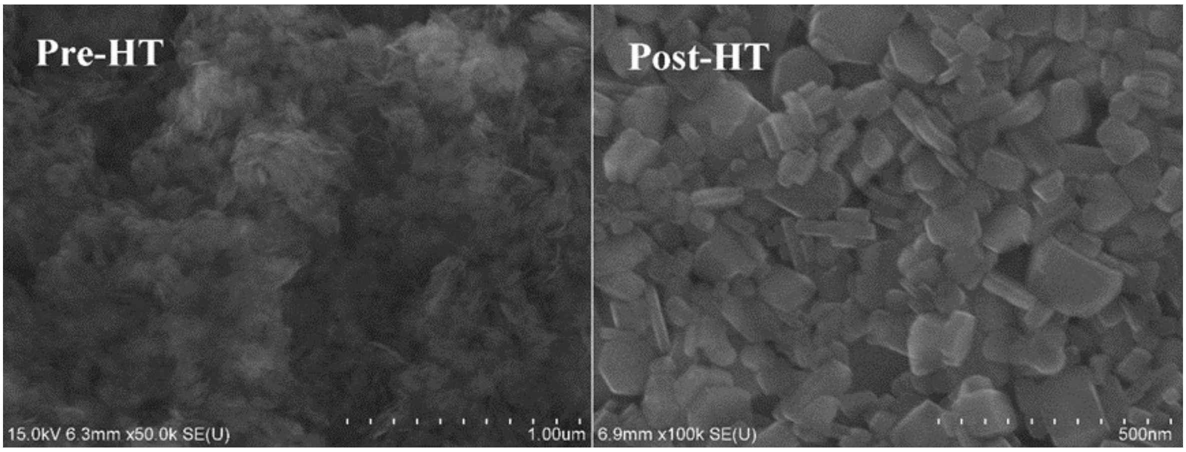

Fig. S2 XRD patterns of gamma Al_2O_3 before (black line) and after (red line, PDF No. 01-083-1505) hydrothermal testing (HT), and their average particle size; SEM images of the pre- and post-HT samples.

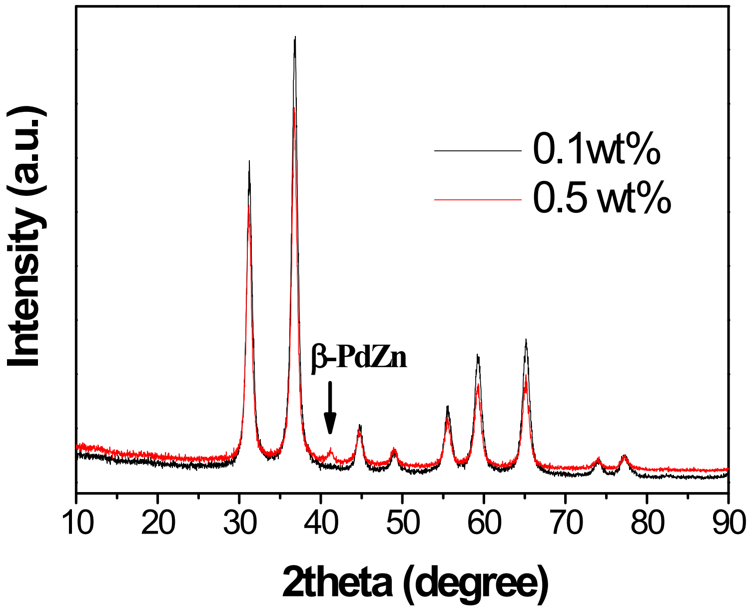

Fig. S3 XRD patterns of 0.1wt%PdZn/$ZnAl_2O_4$ and 0.5wt%PdZn/$ZnAl_2O_4$ catalysts.

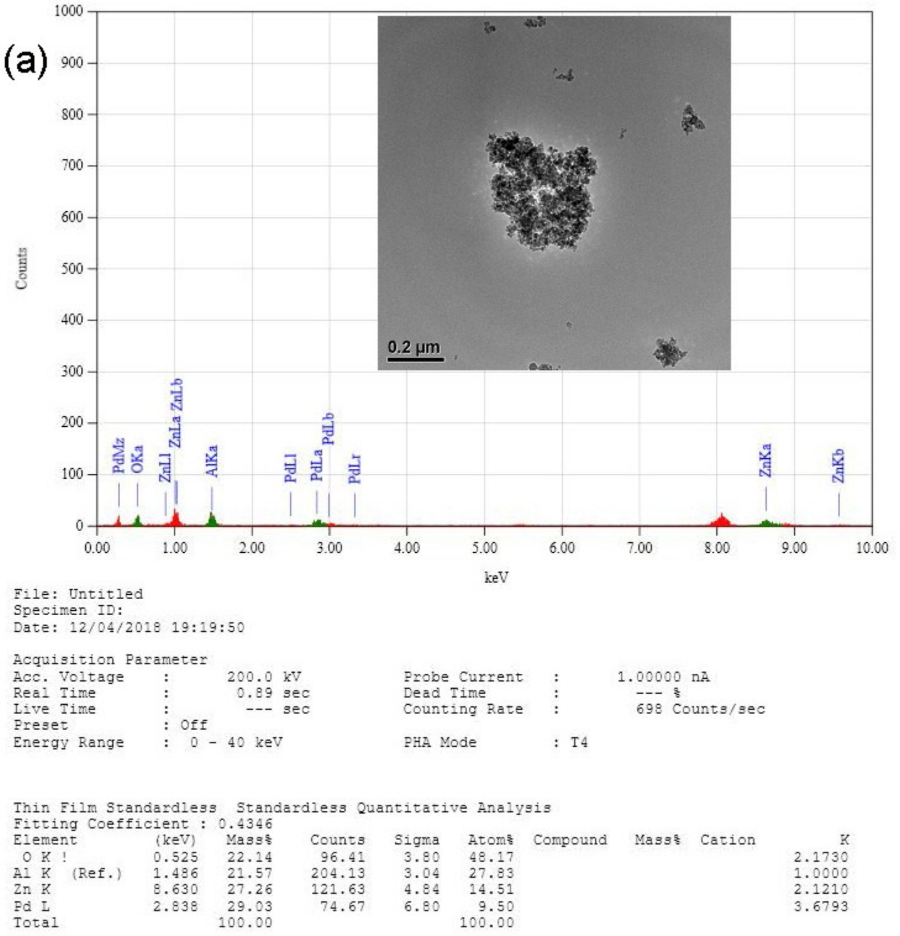

```
File: Untitled
Specimen ID:
Date: 12/04/2018 19:19:50

Acquisition Parameter
Acc. Voltage     :       200.0 kV          Probe Current    :       1.00000 nA
Real Time        :        0.89 sec         Dead Time        :         --- %
Live Time        :         --- sec         Counting Rate    :         698 Counts/sec
Preset           : Off
Energy Range     :   0 - 40 keV            PHA Mode         : T4


Thin Film Standardless  Standardless Quantitative Analysis
Fitting Coefficient : 0.4346
Element          (keV)    Mass%    Counts    Sigma    Atom%  Compound   Mass%  Cation          K
 O K !           0.525    22.14     96.41     3.80    48.17                               2.1730
Al K  (Ref.)     1.486    21.57    204.13     3.04    27.83                               1.0000
Zn K             8.630    27.26    121.63     4.84    14.51                               2.1210
Pd L             2.838    29.03     74.67     6.80     9.50                               3.6793
Total                    100.00                      100.00
```

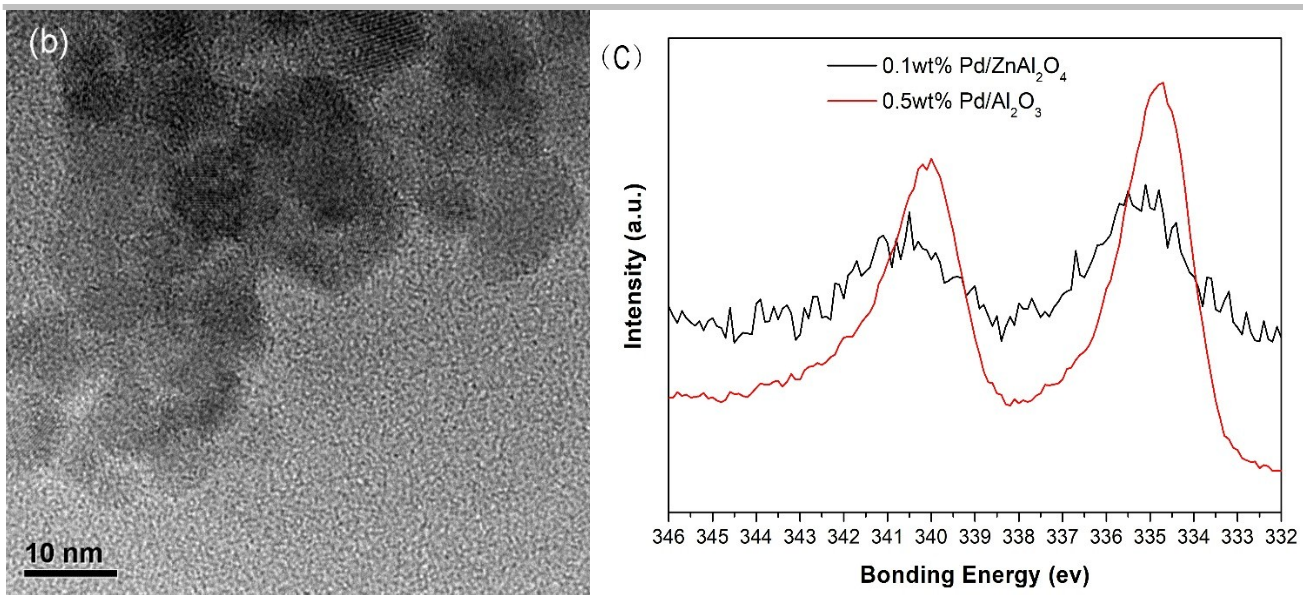

Fig. S4 TEM and EDX (a) , HRTEM image (b), and XPS results of the 0.1wt%PdZn/ZnAl$_2$O$_4$ catalysts.

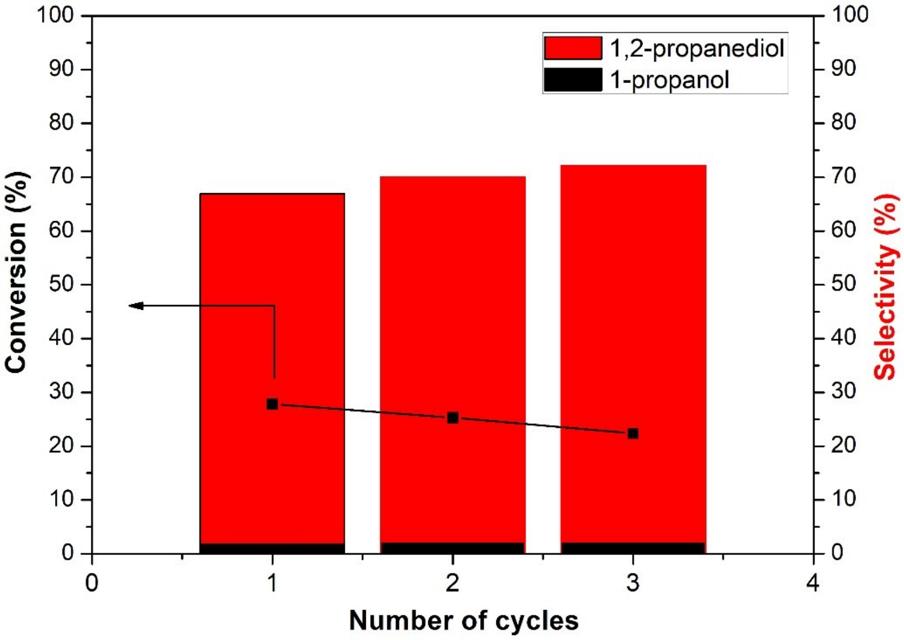

Fig. S5 Conversions of glycerol and selectivity to 1,2-PDO for three consecutive cycles of the glycerol hydrogenolysis on PdZn/ZnAl$_2$O$_4$ catalysts with 0.1wt% Pd loading on the Al-rich spinel support (1.0 g Cat., 473 K, 3.0 MPa H$_2$, 4 h, 10 wt % aqueous glycerol solution).

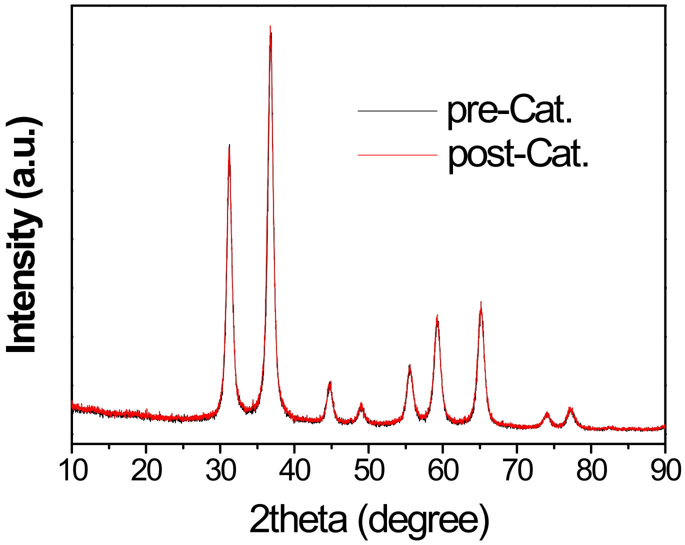

samples	Formula	Wt %
Fresh	Al_2O_3	54.82
	ZnO	45.08
	Pd	0.10
Spent	Al_2O_3	56.02
	ZnO	43.85
	Pd	0.13

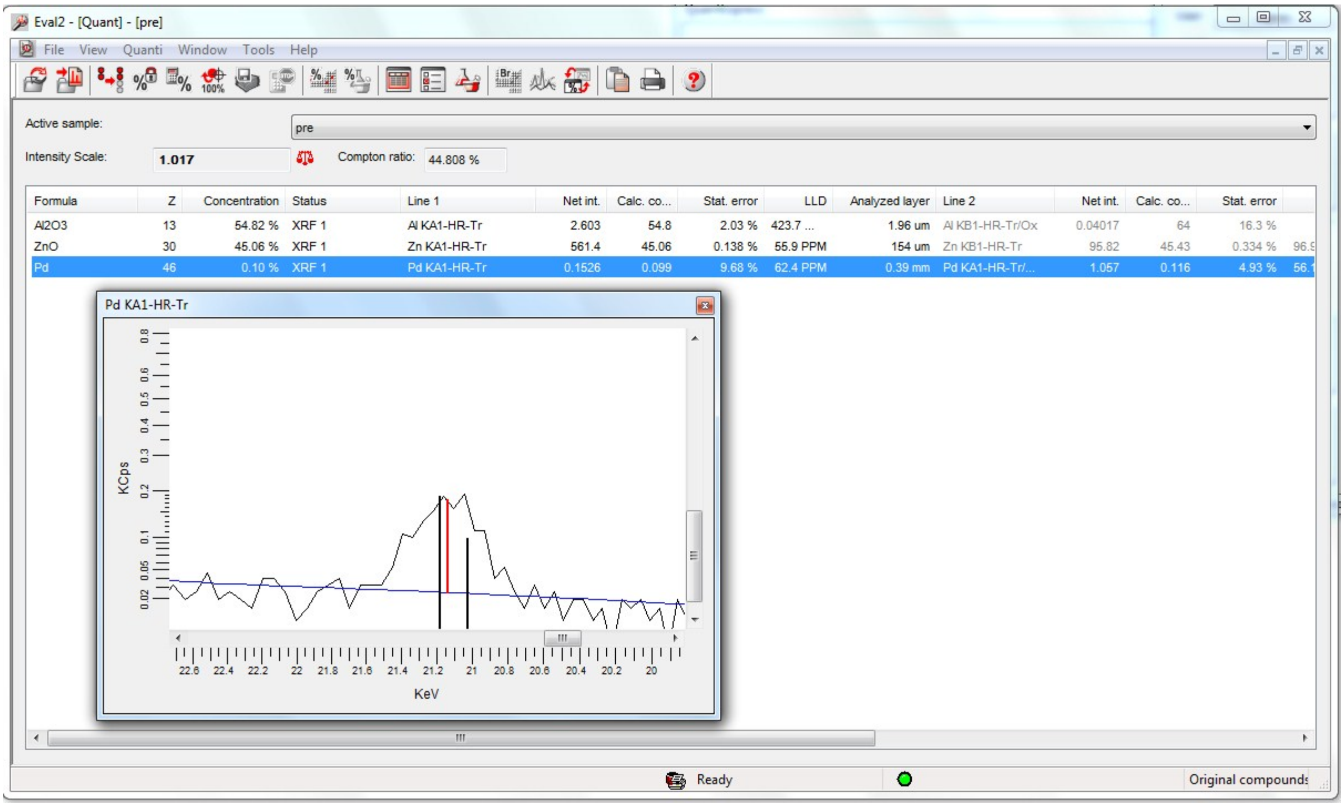

Active sample: pre

Intensity Scale: 1.017

Compton ratio: 44.808 %

Formula	Z	Concentration	Status	Line 1	Net int.	Calc. co...	Stat. error	LLD	Analyzed layer	Line 2	Net int.	Calc. co...	Stat. error	
Al2O3	13	54.82 %	XRF 1	Al KA1-HR-Tr	2.603	54.8	2.03 %	423.7 ...	1.96 um	Al KB1-HR-Tr/Ox	0.04017	64	16.3 %	
ZnO	30	45.06 %	XRF 1	Zn KA1-HR-Tr	561.4	45.06	0.138 %	55.9 PPM	154 um	Zn KB1-HR-Tr	95.82	45.43	0.334 %	96.9
Pd	46	0.10 %	XRF 1	Pd KA1-HR-Tr	0.1526	0.099	9.68 %	62.4 PPM	0.39 mm	Pd KA1-HR-Tr/...	1.057	0.116	4.93 %	56.1

Fig. S6 XRD patterns of 0.1wt% $PdZn/ZnAl_2O_4$ catalysts and their XRF data before and after catalytic testing in the hydrogenolysis of glycerol.

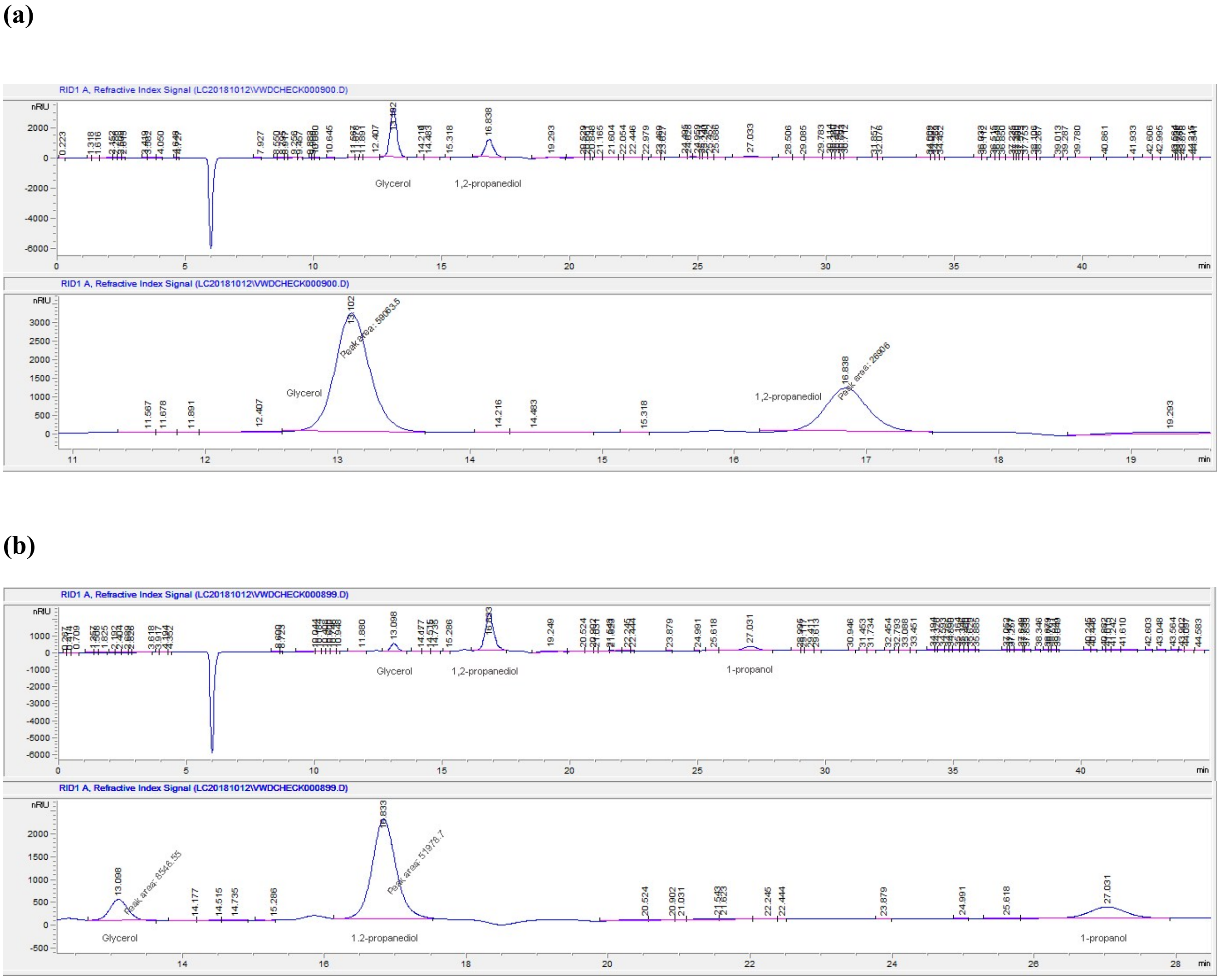

Fig. S7 Chromatograms for the analysis of hydrogenolysis products of glycerol by (a) 0.1wt% $PdZn/ZnAl_2O_4$ catalysts and (b) 0.5wt% $PdZn/ZnAl_2O_4$ catalysts, the top choromatogram is the whole flow, and the bottom showed the peak magnifications.

References

[1] a) G. Kresse, J. Hafner, *Phys. Rev. B* **1994**, *49*, 14251-14269; b) G. Kresse, J. Furthmuller, *Phys. Rev. B* **1996**, *54*, 11169-11186; c) G. Kresse, J. Joubert, *Phys. Rev. B* **1999**, *59*, 1758-1775.

[2] Y.-S. Kim, K. Hummer, G. Kresse, *Phys. Rev. B* **2009**, *80*, 035203.

[3] J. P. Perdew, K. Burke, M. Ernzerhof, *Phys. Rev. Lett.* **1996**, *77*, 3865-38.